Molecular Organization of the Complex between the Muscarinic M3 Receptor and the Regulator of G Protein Signaling, Gβ 5 −RGS7

ARTICLE *in* BIOCHEMISTRY · JUNE 2010

Impact Factor: 3.02 · DOI: 10.1021/bi100080p · Source: PubMed

5 AUTHORS, INCLUDING:

Simone Sandiford
Johns Hopkins Bloomberg School of Public …
10 PUBLICATIONS **271** CITATIONS
SEE PROFILE

Konstantin Levay
University of Miami Miller School of Medicine
26 PUBLICATIONS **762** CITATIONS
SEE PROFILE

Peter Buchwald
University of Miami Miller School of Medicine
121 PUBLICATIONS **1,942** CITATIONS
SEE PROFILE

4998 *Biochemistry* **2010,** *49,* 4998–5006
DOI: 10.1021/bi100080p

BIOCHEMISTRY
including biophysical chemistry & molecular biology
Article

Molecular Organization of the Complex between the Muscarinic M3 Receptor and the Regulator of G Protein Signaling, $G\beta_5$−RGS7[†]

Simone L. Sandiford, Qiang Wang, Konstantin Levay, Peter Buchwald, and Vladlen Z. Slepak*

Department of Molecular and Cellular Pharmacology, University of Miami Miller School of Medicine, Miami, Florida 33136

Received January 19, 2010; Revised Manuscript Received April 12, 2010

ABSTRACT: The complex of the regulator of G protein signaling (RGS), $G\beta_5$−RGS7, can inhibit signal transduction via the M3 muscarinic acetylcholine receptor (M3R). RGS7 consists of three distinct structural entities: the DEP domain and its extension DHEX, the Gγ-like (GGL) domain, which is permanently bound to Gβ subunit $G\beta_5$, and the RGS domain responsible for the interaction with Gα subunits. Inhibition of the M3R by $G\beta_5$−RGS7 is independent of the RGS domain but requires binding of the DEP domain to the third intracellular loop of the receptor. Recent studies identified the dynamic intramolecular interaction between the $G\beta_5$ and DEP domains, which suggested that the $G\beta_5$−RGS7 dimer could alternate between the "open" and "closed" conformations. Here, we identified point mutations that weaken DEP−$G\beta_5$ binding, presumably stabilizing the open state, and tested their effects on the interaction of $G\beta_5$−RGS7 with the M3R. We found that these mutations facilitated binding of $G\beta_5$−RGS7 to the recombinant third intracellular loop of the M3R but did not enhance its ability to inhibit M3R-mediated Ca^{2+} mobilization. This led us to the idea that the M3R can effectively induce the $G\beta_5$−RGS7 dimer to open; such a mechanism would require a region of the receptor distinct from the third loop. Indeed, we found that the C-terminus of M3R interacts with $G\beta_5$−RGS7. Truncation of the C-terminus rendered the M3R insensitive to inhibition by wild-type $G\beta_5$−RGS7; however, the open mutant of $G\beta_5$−RGS7 was able to inhibit signaling by the truncated M3R. The GST fusion of the M3R C-tail could not bind to wild-type $G\beta_5$−RGS7 but could associate with its open mutant as well as with the separated recombinant DEP domain or $G\beta_5$. Taken together, our data are consistent with the following model: interaction of the M3R with $G\beta_5$−RGS7 causes the DEP domain and $G\beta_5$ to dissociate from each other and bind to the C-tail, and the DEP domain also binds to the third loop, thereby inhibiting M3R-mediated signaling.

G protein-coupled receptors (GPCRs)[1] mediate many physiological processes, including neuronal transmission and hormonal regulation. According to the classical model of GPCR signaling, an activated receptor interacts with a heterotrimeric G protein, causing the exchange of GDP bound to the G protein α subunit (Gα) for GTP (*1*, *2*). Binding of GTP results in the dissociation of Gα from the G$\beta\gamma$ complex (*3*), and both Gα-GTP and G$\beta\gamma$ influence activities of effector enzymes or ion channels (*4*−*6*). The return of the GPCR-mediated pathway to its basal state involves hydrolysis of GTP by the G protein. For most G proteins, rapid GTP hydrolysis requires participation of regulators of G protein signaling (RGS), which act as GTPase activating proteins (GAPs) for Gα subunits. More than 30 mammalian RGS proteins have been discovered. Outside of the conserved 120-amino acid RGS domain that is responsible for the GAP activity, RGS proteins are very diverse, ranging from ∼25 to 120 kDa. According to this diversity, they are classified into distinct subfamilies (reviewed in refs (*7*−*11*)).

[†]Supported by National Institutes of Health Grant GM 060019 (V.Z. S.).

*To whom correspondence should be addressed: 1600 NW 10th Ave., Miami, FL 33136. Phone: (305) 243-3430. Fax: (305) 243-4555. E-mail: v.slepak@miami.edu.

[1]Abbreviations: RGS, regulator of G protein signaling; R7BP, R7 family RGS protein binding protein; GPCR, G protein-coupled receptor; GST, glutathione *S*-transferase; CFP and YFP, cyan and yellow versions, respectively, of green fluorescent protein (GFP); CHO, Chinese hamster ovary; PCR, polymerase chain reaction.

The R7 family of RGS proteins (RGS6, -7, -9, and -11) is defined by the presence of the N-terminal DEP and DHEX domains [Dishevelled, Egl10, Pleckstrin (DEP), and DEP helical extension, respectively], the centrally located GGL domain (Gγ-like), and the C-terminal RGS domain (*12*−*14*). The GGL domain associates permanently with G protein β subunit $G\beta_5$ (*15*−*17*). The DEP domain binds to R7BP (R7 binding protein), a palmitoylated neuronal protein that can recruit $G\beta_5$−R7 dimers to the plasma membrane (*18*−*20*). Biochemical studies and crystallography showed that the DEP domain and the Gβ5 subunit also bind to each other (*21*, *22*).

R7 proteins are implicated in the regulation of neuronal processes such as sensory transduction, locomotor activity, and addiction (*23*). At the molecular level, their function is primarily associated with negative regulation of the Gi family of G proteins. It was shown that R7 proteins do not possess GAP activity for Gq in vitro (*24*). However, in *Caenorhabditis elegans*, the R7 protein EAT-16 antagonizes the function of Egl-30, the ortholog of Gq (*25*−*27*), and in transfected mammalian cells RGS7 was shown to downregulate signaling via the Gq-coupled muscarinic M3 receptor, M3R (*21*, *28*, *29*). In a recent report, we showed that this regulation occurs via a novel mechanism that does not require GAP activity but instead involves direct binding of the RGS7 DEP domain to the third intracellular loop of the M3R (M3Ri3) (*30*). In the M3R, this loop is unusually long (more than 200 amino acids) and was previously shown to interact with

 Published on Web 05/05/2010

multiple proteins, including G_q (*31*), β-arrestins (*32*), Gβγ subunits (*33*, *34*), calmodulin (*35*), and the phosphatase inhibitor SET (*36*), and to contain phosphorylation sites for several kinases (*37*, *38*).

In this study, we sought to investigate the significance of the DEP−Gβ$_5$ intramolecular interaction in the association of the Gβ$_5$−RGS7 complex with the M3R.

MATERIALS AND METHODS

Reagents and Antibodies. Fura-2AM was obtained from Invitrogen. Unless otherwise noted, all chemicals were obtained from Sigma. Rabbit RGS7 (1:1000), Gβ$_5$ (1:1000), and Gβ$_1$ (1:10000) antibodies have been described previously (*28*). Anti-Flag-M2 HRP conjugate was from Sigma (1:5000) and mouse anti-GFP antibody JL-8 was from Clontech (1:1000). Anti-rabbit (1:5000) and anti-mouse (1:3000) secondary antibodies conjugated to peroxidase were from Jackson Laboratories. Anti-rabbit fluorescein-labeled antibodies (1:400) were from Amersham Biosciences, and the anti-mouse Cy3-labeled antibody (1:400) was from Sigma.

Cell Culture, Transfection, and Lysate Preparation. CHO-K1 cells were cultured in F-12K Nutrient Mixture (Kaighn's modification) with 10% FBS and penicillin/streptomycin and plated at a density of $0.8-1.0 \times 10^6$ cells per 100 mm plate 24 h prior to transfection. Transfection was conducted using Lipofectamine (Invitrogen) in accordance with the manufacturer's instructions, as described previously (*28*). The ratio of RGS7 to Gβ$_5$ DNA was maintained at 5:1, with a total of 8.0 μg of DNA per plate. LacZ DNA was used as a control to ensure that the total DNA per plate remained constant.

After transfection, cells were washed with PBS and lysed in hypotonic buffer [5 mM Tris-HCl (pH 7.6), 0.1 mM $MgCl_2$, 1 mM DTT, and protease inhibitor cocktail (Roche)]. Cells were frozen and thawed twice and centrifuged at 14000 rpm for 45 min. The supernatant (total protein concentration of 1.0−1.5 mg/mL) represented the cytosolic fraction and was used for the pull-down assays involving cytosolic proteins.

Cloning of GST Fusion Proteins. The following GST fusion constructs were generated for bacterial expression and subsequent purification for use in the GST pull-down assay.

(*i*) *R7-DEP*. Nucleotides 100−372 (corresponding to amino acids 34−124 of bovine RGS7) were PCR amplified from the full-length RGS7 cDNA and cloned into the pGEX-KG vector, as previously described (*21*). The mutant forms of the GST−DEP constructs were also generated by PCR-mediated mutagenesis utilizing the primers containing the desired substitutions. The RGS7 amino acids were substituted with the corresponding RGS9 residues in the K52S mutant and triple mutants K52S/E73S/D74G and D29A/R33D/K38D. RGS7 residues were substituted with alanine in the F57A mutant and double mutants F49A/L50A and F107A/F110A. All these R7-DEP mutants were cloned into the pGEX-KG vector linearized with BstBI and HindIII.

(*ii*) *Third Intracellular Loop of the M3 Receptor, GST−M3Ri3*. The GST fusion of the third intracellular loop of the human muscarinic M3 receptor (amino acids 345−390) was described previously (*30*).

(*iii*) *C-Termini of Muscarinic Receptors*. The DNA fragment encoding the M3R C-terminus (Asn^{548}−Leu^{590}) was amplified from the full-length human M3R and cloned into the pGEX-2T vector at the BamHI and EcoRI sites. The PCR fragments corresponding to the C-terminal amino acid residues of the human M1R (Asn^{422}−Cys^{460}) and M5R (Asn^{499}−Pro^{532}) were cloned in the same manner.

Constructs for Expression in Mammalian Cells. $RGS7^{249-469}$: This RGS7 construct, described before (*21*) lacks the DEP and DHEX domains of RGS7 and was generated by PCR amplification of nucleotides 745−1410 (corresponding to amino acids 249−469). The fragment was incorporated into the pcDNA3.0 vector linearized with *Bam*HI and NotI.

(*i*) *YFP-R7*. RGS7 cDNA was cloned into the pEYFP-C1 vector and has been previously described (*29*).

(*ii*) $RGS7^{ED/SG}$. The double mutation E73S/D74G was introduced into full-length RGS7 using the same primers used for creation of the GST fusion of the E73S/D74G R7-DEP double mutant (*21*).

(*iii*) $YFP\text{-}R7^{F107A/F110A}$. RGS7 cDNA was cloned into the pEYFP-C1 vector at the BglII and HindIII sites. The F107A/F110A double mutation was introduced using the same primers used for the generation of the F107A/F110A R7-DEP mutant.

(*iv*) *YFP-DEP*. Nucleotides 1−372 corresponding to the N-terminus and the DEP domain of bovine RGS7 were PCR amplified from full-length RGS7 and cloned into the pEYFP-C1 vector at the BglII and HindIII sites, as previously described (*30*).

Gβ$_5$ Mutants. Gβ$_5$ cDNA was cloned into the pcDNA3.0 vector at the BamHI and NotI sites. Gβ$_5$ mutants K54A, R56A/R57A, K60A, H62A, W107A, D259A, I282A/I283A, and F284A were generated by substitution of the named amino acids with alanines using primers containing the mutations. The PCR-generated fragments were then cloned into the pcDNA3.0 vector at the BamHI and NotI sites.

The CFP−Gβ$_5$ construct has been previously described (*29*, *39*).

Truncated M3R (*M3R-ΔC*). The human M3R construct that lacks most of the C-terminus was produced by introduction of a stop codon at position 565 as previously described (*40*) and was kindly provided by A. Tobin (University of Leicester, Leicester, U.K.).

GST Pull-Down Assay. The GST pull-down assays were performed as previously described with minor modifications (*21*, *30*). Glutathione Sepharose 4B beads were prewashed with PBS and 0.1% CHAPS and incubated at 4 °C with purified GST or the GST fusion proteins for 1−2 h. Purified GST or a GST fusion protein was immobilized on the matrix at a ratio of 0.15−0.3 μg/μL of packed resin; the amount of immobilized protein was determined with a Bradford protein assay (Pierce) and verified by SDS−PAGE stained by Coomassie. After three washes with PBS and 0.1% CHAPS, the slurry was mixed with the cell lysates required by the experiment and incubated overnight at 4 °C on a rotary shaker. At the end of the incubation, the agarose beads were settled by gravity and the supernatant was collected as the unbound fraction. The resin was extensively washed with PBS and 0.1% CHAPS and then eluted with SDS-containing sample buffer. In a typical assay, the packed volume of the resin was 30 μL, and the volume of the protein lysate was 300 μL. The beads were washed three times with 600 μL of PBS and 0.1% CHAPS buffer and eluted with 30 μL of 2× SDS−PAGE sample loading buffer. The input (total cell lysate), unbound, and eluted fractions were resolved on a 10% SDS gel and analyzed by Western blotting. In routine experiments in which only 5−20% of the protein subjected to the pull-down assay was captured by the beads (i.e., using the GST fusions of the M3R fragments) and there was no appreciable difference

between the total and unbound fractions, we analyzed only the unbound and eluted material.

Calcium Mobilization Assay. The cDNA clone for the human muscarinic M3 receptor was obtained from the Missouri S&T cDNA Resource Center (www.cdna.org). CHO-K1 or CHO-R7BP (*30*) cells were transiently transfected and plated on 12 mm glass coverslips (Electron Microscopy Sciences). After being transfected, cells were washed with Hank's buffered saline solution (HBSS) supplemented with 2% FBS and incubated in the same medium containing 1 μM fura-2AM for 45 min at ambient temperature in the dark. The cells were then incubated for 30 min in Locke's buffer (20 mM Hepes, 128 mM NaCl, 5 mM KCl, 1.2 mM Na_2HPO_4, 2.7 mM $CaCl_2$, and 10 mM glucose) to allow de-esterification of fura-2AM. The coverslips were then secured in a flow chamber and mounted on the stage of a Nikon TE2000 inverted fluorescence microscope. The chamber was continuously perfused with Locke's buffer under gravity flow, and cells were stimulated with a carbachol solution in the same buffer.

The images were collected using a 20× UV objective lens every 2 s using Metafluor. The excitation wavelengths were 340 and 380 nm, and the emission was set at 510 nm. The free Ca^{2+} concentration was determined from the fluorescence measurements on the basis of calibration performed with the fura-2 Ca^{2+} imaging kit (Molecular Probes) according to the manufacturer's instructions.

Confocal Microscopy. CHO-K1 or CHO-R7BP cells were plated to achieve a density of 1×10^5 cells on 22 mm glass coverslips placed in a six-well plate. For transient transfection, 1 μg of total plasmid DNA was used per well, and the RGS7:Gβ_5 DNA ratio was maintained at 5:1 for both wild-type and mutant RGS7 and Gβ_5 constructs. Twenty-four hours after transfection, cells were fixed in 4% paraformaldehyde in PBS for 10 min at room temperature, washed twice with PBS, and incubated in blocking solution (1% BSA and 0.1% Triton X-100 in PBS) for 20 min. This was followed by a 1 h incubation with the anti-GFP antibody diluted in blocking solution. CHO-R7BP cells were incubated with anti-Flag antibody for an additional 1 h for detection of the tagged R7BP. Fluorescein and Cy3 secondary antibodies were diluted in blocking solution and used for the detection of green and red fluorescence, respectively. After the samples had been stained, the coverslips were then rinsed thoroughly in PBS and water, then mounted on glass slides using Antifade reagent containing Dapi (Invitrogen), and imaged using a Leica TCS SP5 laser scanning confocal microscope. Images shown represent a single optical plane selected from at least 10 stacks that were taken for each cell.

Protein Structure Modeling. The three-dimensional model of RGS7 was obtained as a homology (comparative) protein structure with SWISS-MODEL and Swiss PdbViewer/Deep View version 3.7 (SP5) (*41*, *42*) using Gβ_5−RGS9 [Protein Data Bank (PDB) entry 2PBI] (*22*) as the template. The alignment between bovine RGS7 and residues 1−422 of mouse RGS9 (*22*) exhibited 36% identity. The first 42 amino acids in the RGS7 model were automatically omitted by the software during the homology fitting procedure to yield a "best fit" model. Images, including three-dimensional ribbon diagrams, were generated using Discovery Studio Visualizer version 1.7 (Accelrys, Inc., San Diego, CA).

RESULTS

Our previous studies showed that the DEP domain of RGS7 was responsible for the inhibition of muscarinic M3 receptor signaling and that the interaction between the DEP domain and the receptor was blocked by the Gβ_5 subunit (*30*). These data led us to hypothesize that the DEP domain can inhibit the M3R once it dynamically dissociates from Gβ_5. The main goal of this study was to test this model by disrupting the DEP−Gβ5 interaction via site-directed mutagenesis and characterization of the interaction of the resulting "open" mutants with the M3R.

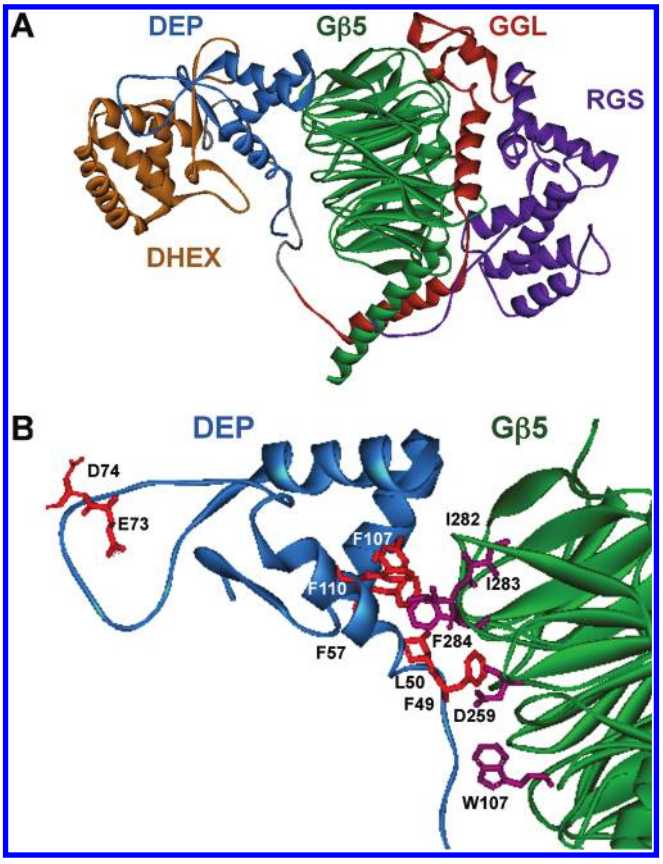

FIGURE 1: Molecular model of the Gβ_5−RGS7 dimer. (A) Ribbon diagram presentation of the homology model of the Gβ_5−RGS7 complex constructed on the basis of PDB coordinates of the crystal structure of the Gβ_5−RGS9-1 complex (*22*). The Gβ_5 polypeptide chain is colored green. The domains of RGS7 are highlighted in the following colors: blue for DEP, light brown for DHEX, red for GGL, and purple for RGS. In this projection, the doughnut-shaped Gβ_5 structure is seen from the side. Gβ_5 makes multiple contacts with the GGL domain, and the Gβ_5/GGL moiety resides between the DEP and RGS domains. The area of contact between the DEP domain and Gβ_5 is shown in more detail in panel B. (B) DEP−Gβ_5 interface. Amino acids that are found within the 1.5 Å radius of the opposite chain are colored red (RGS7) and purple (Gβ_5).

Mutational Analysis of the Interface between the DEP Domain of RGS7 and Gβ_5. Before the Gβ_5−RGS9 crystal structure became available (*22*), we attempted to locate the residues essential for the Gβ_5−DEP interaction through amino acid sequence analysis of different DEP domains and Gβ subunits. We searched for the differences between RGS7, which bound to Gβ_5 in our pull-down assay, and RGS9, which did not (*21*), also taking into consideration the NMR structure of the DEP domain of pleckstrin (*43*). Because both Gβ_5 and Gβ_1 bound to the DEP domain of RGS7, we also screened for positively charged conserved residues in Gβ subunits. We identified a double mutation (E73S/D74G, abbreviated as ED/SG) in the DEP domain of RGS7, which weakened its binding to Gβ_5 (*21*). Other tested mutations (K54A, R56A/R57A, K60A, and H62A in Gβ_5 and D29A/R33D/K38S and K52S in RGS7) had no effect on the Gβ_5−DEP interaction (data not shown).

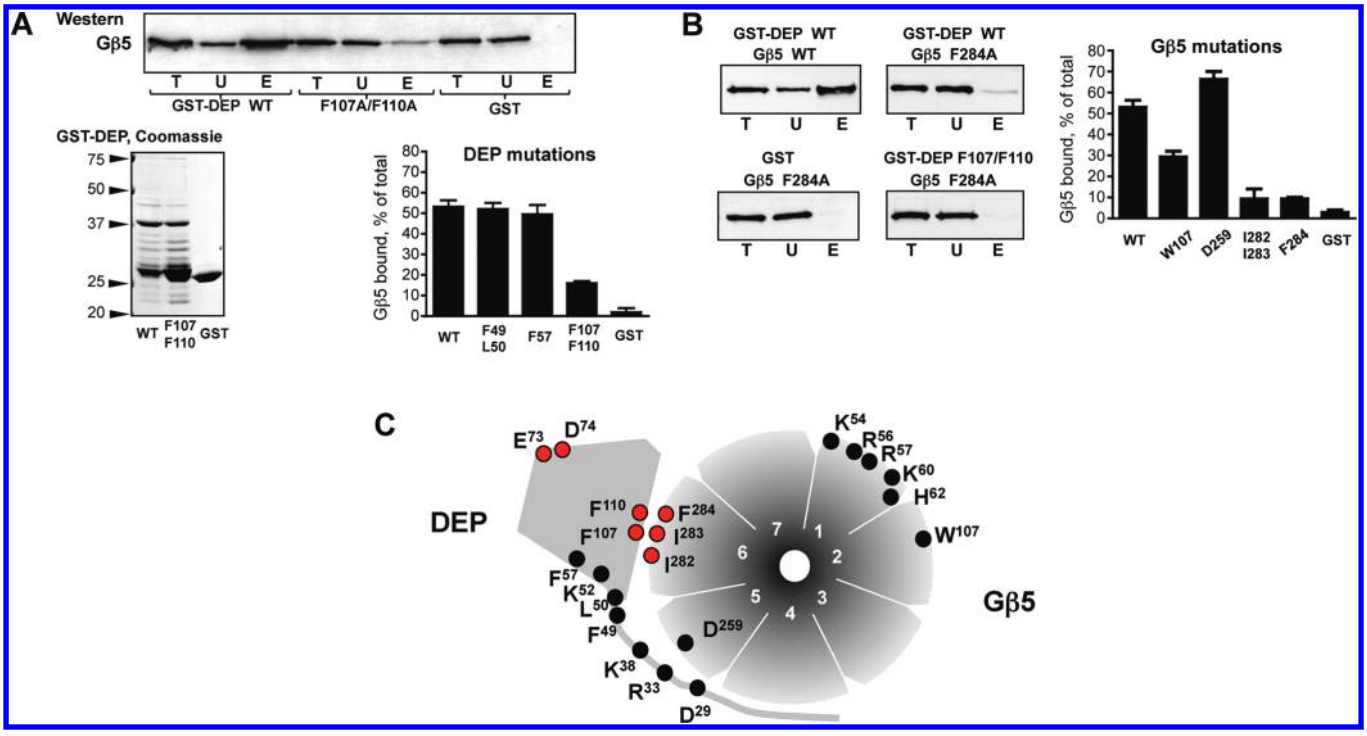

FIGURE 2: Mutational analysis of the DEP−Gβ_5 interface. Indicated amino acids of the RGS7 DEP domain or Gβ_5 were substituted. Residues D29, R33, K38, K52, E73, and D74 were changed to the corresponding RGS9 residues, and all other residues were substituted with alanines, as described in Materials and Methods. (A) Analysis of the RGS7 DEP domain mutants. The DEP domain mutants were expressed as GST fusion proteins and analyzed by SDS−PAGE and Coomassie blue staining. Along with the full-length GST−DEP fusion protein (~38 kDa), these preparations contained apparent degradation products, which were similar among all the DEP mutants. The wild-type and mutant GST−DEP proteins were immobilized on glutathione beads, so that the amounts of the fusion proteins were equal and corresponded to the amount of GST immobilized on the control beads. The complex of wild-type Gβ_5 with the RGS7$^{249-469}$ construct was expressed in CHO-K1 cells by transient transfection, and the cell lysate was subjected to the GST pull-down assay, as described in Materials and Methods. The Western blot panel shows a representative experiment in which the Gβ_5−RGS7$^{249-469}$ complex was tested for binding with the beads containing the GST fusion of the wild-type DEP domain (WT), the double mutant F107A/F110A, or GST. The beads were washed and then eluted with SDS-containing sample buffer. The total CHO-K1 cell lysate (T) and the unbound (U) and eluate (E) fractions were probed with the anti-Gβ_5 antibody, followed by ECL detection. The films were scanned and analyzed with Scion. The bar graph summarizes the quantification of the data obtained from the entire series of experiments with all tested RGS7 DEP mutants. Material in the eluate (E) fractions was 5 times more concentrated than that in the unbound or total fraction, which ensured that the resulting ECL signal was within the linear range of detection. The values of the amount of Gβ_5 present in the analyzed fractions were calculated accordingly and presented as the percentages of Gβ_5 that eluted from the beads relative to the total amount of Gβ5 in the cell lysate. Shown are the mean values with error bars representing the standard deviation from three to six independent experiments. (B) Analysis of Gβ_5 mutations. The indicated Gβ_5 mutants were expressed in CHO cells in a complex with the RGS7$^{249-469}$ construct and tested for their ability to bind to the wild-type GST−DEP fusion protein using the pull-down assay described for panel A. Representative Western blots show the total lysate (T), unbound (U), and eluted (E) fractions analyzed by immunobloting using the antibodies against Gβ_5. The bottom right panel shows the experiment in which the Gβ_5 F284A mutant was tested for binding with the F107A/F110A mutant of the GST−DEP fusion protein. The bar graph depicts quantification of the data from three or four independent experiments with four Gβ_5 mutants (W107A, D259A, F284A, and the I282A/I283A double mutant) binding to the wild-type GST−DEP fusion protein or GST. (C) Diagram summarizing our mutational analysis of Gβ_5 and RGS7. The seven blades of the Gβ_5 "β-propeller" are numbered 1−7. The indicated mutants were tested in the GST pull-down assays described for panels A and B; the E73S/D74G mutation was described in our previous study (*21*). The mutations producing a weaker DEP−Gβ_5 interaction are denoted by the red circles; those without a distinct phenotype are marked with black circles.

The recently determined crystal structure of the Gβ_5−RGS9 dimer (*22*) allowed us to generate a three-dimensional homology model of the Gβ_5−RGS7 complex. As expected, the backbones of RGS7 and RGS9 superimposed very well. Like in the Gβ_5−RGS9 complex, in our model, the Gβ_5 chain interfaces extensively with the GGL domain of RGS7, and the Gβ_5/GGL moiety is sandwiched between the RGS and DEP domains (Figure 1A). We made the assumption that RGS7 and Gβ_5 residues located within 1.5 Å of each other could contribute to the interaction between the two proteins. Amino acid residues F49, L50, F57, F107, and F110 of the RGS7 DEP domain and W107, D259, I282, I283, and F284 of Gβ_5 fit this criterion (Figure 1B). We substituted these amino acids for alanines and then expressed and characterized the resulting mutants in vitro (Figures 2−4).

To study the interaction between RGS7 DEP and Gβ_5 (Figure 2), we used our previously developed pull-down assay (*21*, *30*). The mutants of the DEP domain were expressed as GST fusions in *Escherichia coli*, and the Gβ_5 mutants were expressed in CHO-K1 cells together with the DEP-less C-terminal portion of RGS7 (RGS7$^{249-469}$). Our data show that the double mutation F107A/F110A in the DEP domain leads to a clear weakening of its interaction with Gβ_5. As shown in Figure 2A, more than 50% of the Gβ_5−RGS7$^{249-469}$ complex is bound to the beads containing the wild-type GST−DEP fusion protein, whereas the beads with the F107A/F110A mutant GST−DEP fusion protein could retain only ~12% of the Gβ_5 complex. Other mutations of the DEP domain, F49A/L50A and F57A, did not influence the interaction with Gβ_5. In Gβ_5, substitutions of F284 for alanine and the double mutation I282A/I283A also led to an approximately 5-fold reduction in its ability to bind to the RGS7 DEP domain (Figure 2B). The W107A mutation weakened the Gβ_5−DEP interaction approximately 2-fold, whereas the D259A

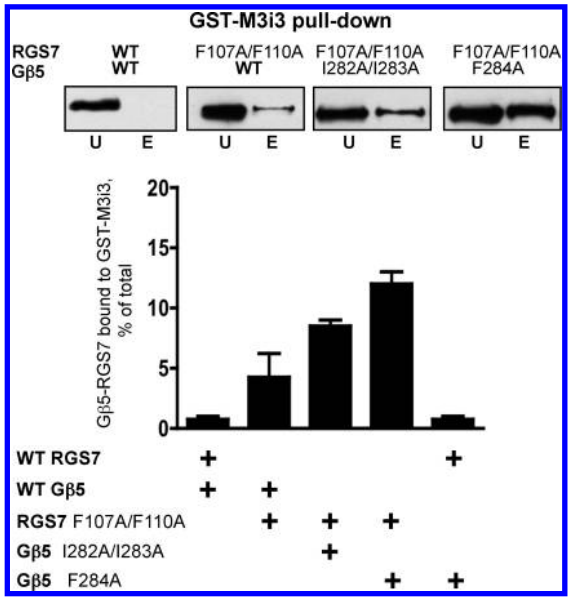

FIGURE 3: Interaction of the open mutants of the $G\beta_5$−RGS7 complex with the third intracellular loop of the M3R. The GST fusion of M3Ri3 was immobilized on the glutathione beads. Wild-type or mutant RGS7 constructs were expressed in CHO-K1 cells as full-length proteins fused to the C-terminus of YFP, together with wild-type or mutant $G\beta_5$. The cell lysates were subjected to the GST pull-down assay. Following the incubation with the beads, the unbound and eluted material was analyzed by Western blotting using the anti-YFP antibody. The different combinations of WT and mutant constructs used are indicated above the four representative immunoblot panels. The amount of RGS7 bound to the M3i3 beads was determined as the fraction of the total amount of RGS7 in the cell lysate. The total was calculated as the sum of the signal in the unbound and eluted fractions, as described in Materials and Methods. The data show the mean and standard deviation from three or four independent experiments.

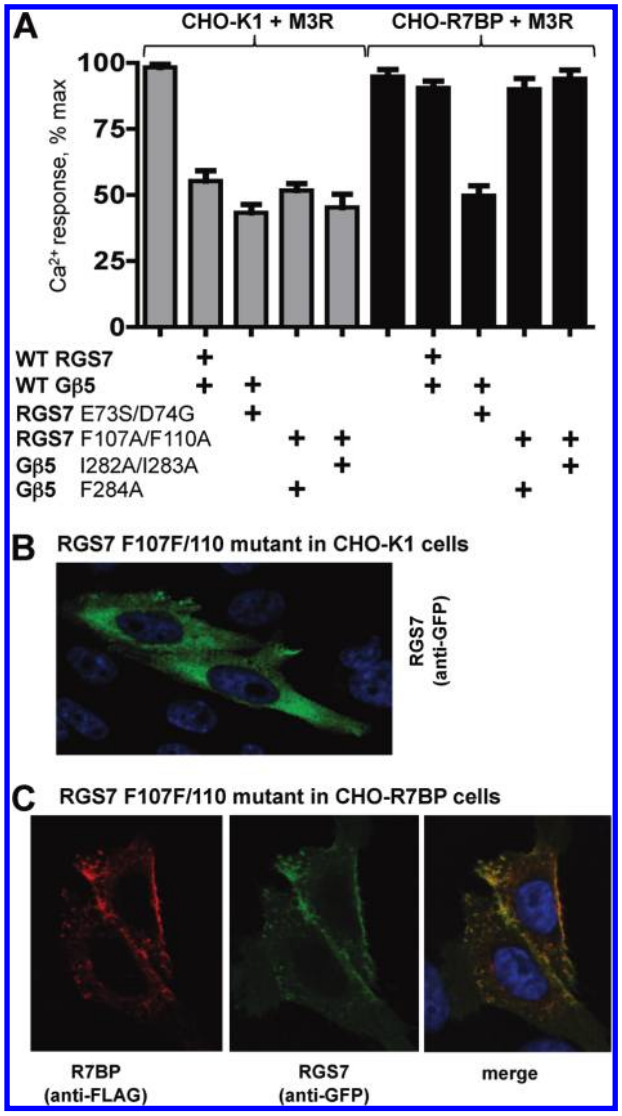

FIGURE 4: Effect of open mutations and R7BP on $G\beta_5$−RGS7 complex-mediated inhibition of M3R signaling. (A) The stable cell line expressing Flag-tagged R7BP (CHO-R7BP, black bars) was transfected with the M3R together with plasmids encoding the indicated mutants or wild-type $G\beta_5$ and RGS7. CHO-K1 cells (gray bars) were used as the control lacking R7BP. The transfected cells were analyzed to determine the peak Ca^{2+} responses to application of 100 μM carbachol, as described in Materials and Methods. The data represent the means ± standard deviation of the peak Ca^{2+} response measured in four independent transfection experiments. (B) CHO-K1 cells were cotransfected with plasmids encoding the F284A mutant of $G\beta_5$ and the F107A/F110A mutant of RGS7, which was fused to the C-terminus of YFP. The cells were then fixed and stained with anti-GFP antibody (1:1000) as described in Materials and Methods. Blue shows staining with Dapi to localize the cell nuclei. (C) The F284A mutant of $G\beta_5$ and the F107A/F110A mutant of RGS7 were co-expressed, via transient transfection, in the stable CHO cell line expressing Flag-tagged R7BP. As in panel B, the RGS7 mutant was expressed as the YFP fusion protein. The cells were fixed and stained with anti-GFP antibody (1:1000) to detect the localization of the $G\beta_5$−RGS7 complex (green) and anti-Flag antibody (1:1000) to detect R7BP (red).

mutation in $G\beta_5$ slightly (~10%) increased the fraction of the $G\beta_5$−$RGS7^{249-469}$ complex absorbed onto the beads with the immobilized wild-type GST−DEP domain. We also tested association of the $G\beta_5$ F284A mutant with the F107A/F110A mutant of the GST−DEP fusion protein and found that the simultaneous mutation of both partners weakened their interaction to the level of nonspecific binding (Figure 2B).

The diagram presented in Figure 2C summarizes all our data for the mutational analysis of the $G\beta_5$−DEP interaction. In our previous study, we identified residues E73 and D74 of RGS7 as being important for association of the DEP domain of RGS7 with the $G\beta_5$ moiety (*21*). We have now found that residues F107 and F110 of the DEP domain and three adjacent hydrophobic residues of $G\beta_5$, I282, I283, and F284, also contribute to the interaction.

Role of $G\beta_5$−DEP Association in the Interaction of the $G\beta_5$−RGS7 Complex with the M3R. Our previous studies suggested that the $G\beta_5$−RGS7 complex binds to the receptor only when it is in its open conformation, i.e., when $G\beta_5$ does not sequester the DEP domain (*30*). This idea implied that mutations destabilizing the $G\beta_5$−DEP interaction should facilitate the transition of the $G\beta_5$−RGS7 dimer toward its open conformation, thereby promoting its interaction with the receptor.

We introduced the F107A/F110A double mutation into the full-length RGS7 cDNA, co-expressed this construct with $G\beta_5$ in CHO-K1 cells, and tested it in the pull-down assay with the GST fusion of the third intracellular loop of the M3R (Figure 3). In contrast to the dimer composed of wild-type RGS7 and $G\beta_5$, this mutant could readily bind to immobilized M3Ri3. $G\beta_5$ mutants F284A and I282A/I283A, when combined with wild-type RGS7, could not bind to the M3Ri3 loop. However, $G\beta_5$ mutations I282A/I283A and particularly F284A augmented the effect of the F107A/F110A mutation of RGS7. These results corroborate the involvement of residues F107 and F110 of the DEP domain and

I282, I283, and F284 of Gβ_5 in the DEP−Gβ_5 interaction (Figures 1 and 2). More importantly, they are consistent with the idea that the transition of the Gβ_5−RGS7 dimer to its open conformation facilitates its interaction with the M3R.

In a parallel series of experiments, we tested whether the mutants displaying stronger binding to the M3Ri3 loop (i.e., open mutants) were also more effective as inhibitors of M3R signaling. Figure 4A shows the effect of the different open mutants of the Gβ_5−RGS7 complex on M3R-mediated Ca^{2+} mobilization elicited by 100 μM carbachol. Contrary to our expectations, the extent of the inhibition conferred by the open mutants was similar to that of the wild-type Gβ_5−RGS7 dimer. Recently, we showed that the Gβ_5−RGS7 complex could reduce the amplitude of the Ca^{2+} response to M3R stimulation by up to 90% if the carbachol concentration was below its K_d (*30*). Under such conditions, the amplitude of the Ca^{2+} response is ~4 times lower compared to the amplitude of the response at 100 μM carbachol, which reduces the overall signal-to-noise ratio, but the inhibitory effect of the Gβ_5−RGS7 complex on M3R signaling has a wider dynamic range. We tested the open mutants at 1 μM carbachol but did not detect a difference between the effect of wild-type and mutant Gβ_5−RGS7 complexes (data not shown). Our earlier study showed that R7BP precluded the wild-type Gβ_5−RGS7 complex from inhibiting M3R signaling, whereas the ED/SG mutant was able to inhibit the M3R even in the presence of R7BP (*21*). Therefore, we expected that the Gβ_5−DEP interface mutations identified in this study could also overcome the effect of R7BP and tested the function of the new open mutants in the presence of R7BP. To limit the number of transfected cDNAs to three (M3R, Gβ_5, and RGS7), we used the previously constructed CHO cell line that stably expresses Flag-tagged R7BP (*21*). Like the wild-type Gβ_5−RGS7 complex, the open mutants localized to the plasma membranes in the cells (Figure 4B), indicating that these mutations did not hamper the ability of the RGS7 complex to bind to R7BP. We found that in contrast to the ED/SG mutant, the complexes composed of RGS7 F107A/F110A and Gβ_5 I282A/I283A or F284A mutants behaved like the wild-type Gβ_5−RGS7 complex both in the absence and in the presence of R7BP.

Thus, whereas the pull-down assay with the M3Ri3 loop revealed a clear difference between the open mutants identified in this study and the wild-type Gβ_5−RGS7 complex (Figure 3), the signaling assay with the full-length receptor did not (Figure 4). To explain the apparent discrepancy between the two experiments, we reasoned that the signaling assay involved an additional factor that was absent in the pull-down experiment. The role of this hypothetical factor would be to facilitate the shift of the Gβ_5−RGS7 complex to its open conformation, so that the wild-type dimer becomes as effective in interacting with the receptor as its open mutants. We proposed that such a factor was a region of the M3R, which is present in the full-length receptor but is absent in the third loop.

The C-Terminus of the M3R Plays a Role in the Interaction with the Gβ_5−RGS7 Complex. Since the first and second loops of the M3R are short, we expected the C-tail of the receptor to be a more likely candidate region for the interaction with the Gβ_5−RGS7 complex. To test this hypothesis, we used two complementary approaches. In one series of experiments (Figure 5), we measured Ca^{2+} responses elicited by the M3R receptor that lacks a portion of its C-terminus (M3R-ΔC). This M3R mutant is truncated by a stop codon at position 565, immediately after the putative helix 8, and was earlier shown to

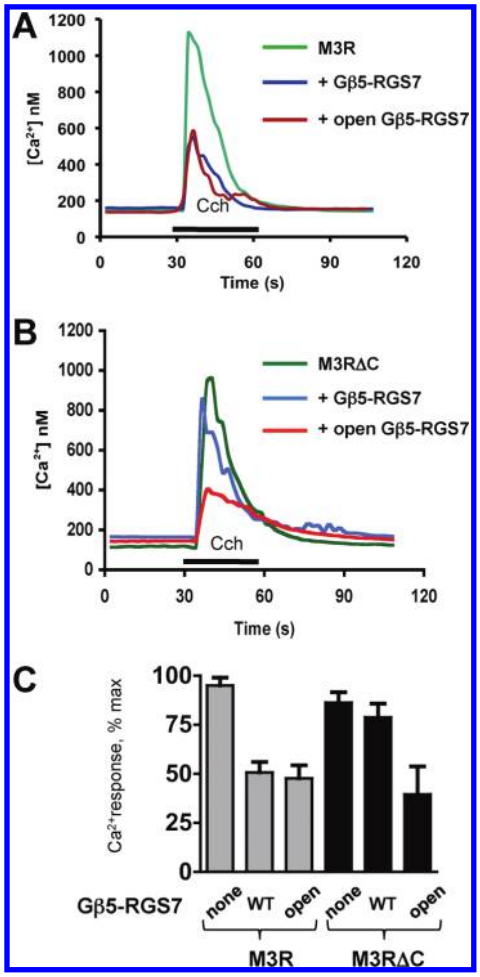

FIGURE 5: C-Terminus of the M3R is essential for the inhibitory action of the Gβ_5−RGS7 complex on M3R signaling. CHO-K1 cells were transiently transfected with M3R, Gβ_5, and RGS7 constructs. Cells were grown on glass coverslips and then loaded with fura-2AM and mounted in a flow chamber at the stage of an inverted fluorescence microscope. Changes in free intracellular Ca^{2+} concentrations in response to stimulation with 100 μM carbachol were recorded in real time from the entire field which contained at least 40 cells, as described in Materials and Methods. The application of carbachol (Cch) is denoted with the black bar. (A) Representative traces from cells transfected with plasmids encoding the M3R and LacZ cDNAs (green), the M3R together with the wild-type Gβ_5−RGS7 complex (blue), or the M3R with the open Gβ_5−RGS7 complex composed of RGS7 F107A/F110A and Gβ_5 F284A mutants (dark red). (B) The M3R construct lacking its C-terminus (M3RΔC) was cotransfected with the wild-type complex or the open mutant of the Gβ_5−RGS7 complex. (C). Quantification of the data from four independent experiments showing the mean ± standard deviation of the peak Ca^{2+} response expressed as the percent of the maximal detected Ca^{2+} response. Gray bars show inhibition of the full-length M3R by the wild-type Gβ_5−RGS7 complex or the open mutant; black bars represent the results with the truncated M3R mutant, M3R-ΔC.

retain the ability to signal via phospholipase C and activate MAP kinases (*40*). In a complementary approach, we tested whether the Gβ_5−RGS7 complex could directly interact with the GST fusion of the M3R C-terminus (M3R-C) (Figure 6).

The Gβ_5−RGS7 complex only marginally reduced the amplitude of the M3R-ΔC-mediated Ca^{2+} response to carbachol, showing that the C-tail is required for the Gβ_5−RGS7 complex to inhibit M3R signaling (Figure 5). However, we found that the open mutant of the Gβ_5−RGS7 complex (Gβ_5 F284A with RGS7 F107A/F110A) could inhibit signaling by the truncated receptor (Figure 5B,C). These results indicate that the C-tail is

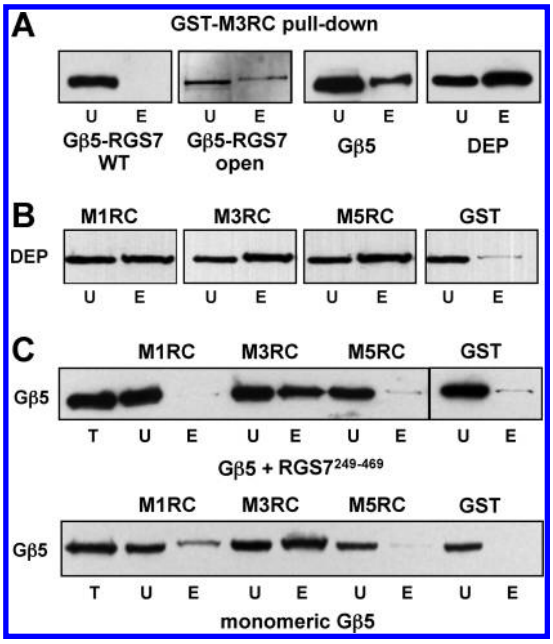

FIGURE 6: C-Terminus of the M3R binds directly to the DEP domain of RGS7, $G\beta_5$, and the open mutant of the $G\beta_5$−RGS7 complex. (A) The C-terminus of the M3R was expressed in *E. coli* as a GST fusion protein and used to pull down the lysates of CHO-K1 cells expressing either the wild-type $G\beta_5$−RGS7 dimer, the $G\beta_5$−RGS7 dimer composed of the RGS7 F107A/F110A and $G\beta_5$ F284A mutants (open mutant), the DEP domain, or $G\beta_5$. In these experiments, RGS7 and $G\beta_5$ were fused to YFP and CFP, respectively, and their presence in the unbound (U) and eluted (E) fractions was detected using an anti-GFP antibody. The pull-down assay was performed as described in Materials and Methods and in a manner similar to that of experiments shown in Figures 2 and 3. (B) The C-termini of muscarinic receptors M1, M3, and M5 were expressed as GST fusion proteins and used to pull down the YFP fusion of the DEP domain of RGS7. Beads with GST were used as a negative control. (C) The GST fusions of the C-termini of M1, M3, and M5 muscarinic receptors were used to pull down the untagged monomeric $G\beta_5$ or its dimer with the $RGS7^{249-469}$ construct. The anti-$G\beta_5$ antibody was used to probe the unbound and eluted fractions in the assays. Each Western blot is representative of at least three independent experiments.

required for inhibition of the M3R by the $G\beta_5$−RGS7 complex and potentially can facilitate the transition of the wild-type $G\beta_5$−RGS7 dimer to its open conformation.

The M3R-C−GST fusion, which included the entire C-tail, did not bind to the wild-type $G\beta_5$−RGS7 dimer but readily bound to the open mutant (Figure 6A). We then asked whether the M3R-C construct could bind to the DEP domain or to $G\beta_5$ and found that, somewhat surprisingly, it could bind to both these entities. Whereas the DEP domain bound to the C-termini of M1, M3, and M5 muscarinic receptors equally well (Figure 6B), monomeric $G\beta_5$ or its complex with the DEP-less $R7^{249-469}$ construct bound selectively to the C-terminus of the M3R (Figure 6C).

These results indicate that the $G\beta_5$−RGS7 complex binds to the M3R via both the third intracellular loop and the C-terminal tail.

DISCUSSION

It is now well appreciated that in addition to G proteins, GPCRs interact with a plethora of partners collectively known as GPCR-interacting proteins (GIPs) (*44*, *45*). These diverse proteins modulate G protein signaling and mediate novel pathways that sometimes even bypass the G proteins. Recently, we reported that muscarinic acetylcholine receptor M3 can directly bind to the regulator of the G protein signaling complex, $G\beta_5$−RGS7, and that this interaction occurs between the DEP domain of RGS7 and the third intracellular loop of the M3R (*30*). In this work, we focus on further investigating the molecular details of this interaction.

The complexes of the R7 family RGS proteins with $G\beta_5$ were discovered more than a decade ago (*15*, *17*), but the significance of their multidomain organization and, above all, the reason why they integrate the $G\beta\gamma$-like entity remained unclear. It was shown that $G\beta_5$ increases the stability of the associated RGS subunit (*28*, *46*), and that the DEP domains play a role in plasma membrane targeting via R7BP (*18*, *19*). However, stability and membrane anchoring can be achieved via other mechanisms; some RGS proteins function while consisting of little more than the RGS box. A hypothesis explaining the significance of the $G\beta_5$−R7 structural organization began to emerge from the finding that the $G\beta_5$ moiety interacts with the DEP domain and, particularly, from the evidence of the dynamic nature of this interaction (*21*). In this model, the dynamic interaction of $G\beta_5$ with the DEP domain enables a functional cycle analogous to the $G\alpha\beta\gamma \leftrightarrow G\alpha + G\beta\gamma$ cycle of heterotrimeric G proteins. As the $G\beta_5$−R7 dimer alternates between the distinct closed and open conformations, it can interact with different binding partners. In this work, we developed this idea further by stabilizing the putative open conformation by introducing mutations that impair the interaction between $G\beta_5$ and the DEP domain.

The first step in our study was to identify the amino acids responsible for the DEP−$G\beta_5$ interaction. On the basis of the homology with the tertiary structure of the $G\beta_5$−RGS9 complex, we identified two phenylalanines (F107 and F110) in the DEP domain of RGS7 and the Ile-Ile-Phe triad in $G\beta_5$ as being important for the interaction (Figures 1 and 2). These amino acids appear to cause the DEP−$G\beta_5$ association through hydrophobic forces. However, other residues may also contribute to this interaction (Figure 2), and as we previously showed, substitution of E73 and D74 in RGS7 with the corresponding Ser and Gly residues of RGS9 (ED/SG mutation) also weakened DEP−$G\beta_5$ binding (*21*). The E73 and D74 residues do not localize at the putative DEP−$G\beta_5$ interface (Figure 1B), making it difficult to explain the phenotype. It is possible that our model of RGS7 is not entirely correct and that the E73 and D74 residues do, in fact, contact the $G\beta_5$ chain. The level of sequence identity between our template (murine RGS9 crystal structure) and target (bovine RGS7) is only 36%, which might be too low for reliable homology modeling. Therefore, the structure of RGS7, especially in solution, can deviate from RGS9 far more than that afforded by the best match algorithm. An alternative explanation is that the ED/SG mutation allosterically influences the position of F107 and F110 at the interface with $G\beta_5$. The ED/SG mutation and the mutations at the DEP−$G\beta_5$ hydrophobic interface result in a clearly distinct phenotype when it is tested in the presence of R7BP (Figure 4). Consistent with our previous report, the ED/SG mutation was able to overcome the negative effect of R7BP on the ability of the $G\beta_5$−RGS7 complex to inhibit M3R signaling. In contrast, open mutants identified in this paper were ineffective in inhibiting M3R signaling in the presence of R7BP (Figure 4A). At the same time, all the mutant forms were capable of binding to R7BP, which was indicated by their ability to localize to the plasma membranes in the R7BP-expressing cells (Figure 4B,C). At the moment, the phenotypic difference between the ED/SG mutant and the new mutations identified in this study

is difficult to explain, and we can only speculate that the ED/SG mutation is more effective in promoting the open conformation.

The idea spurred by our structure−function analysis is that, regardless of how specific mutations impair DEP−Gβ_5 association, they enhance the interaction of the Gβ_5−RGS7 dimer with the M3R. The ED/SG mutation led to a gain of function in terms of inhibition of M3R signaling in the presence of R7BP (*21*) (Figure 4A). Similarly, mutations of the hydrophobic DEP−Gβ_5 interface enabled binding of the Gβ_5−RGS7 to the third intracellular loop (Figure 3) and the C-tail of the M3R (Figure 6) and resulted in the inhibition of the truncated M3R (Figure 5).

In our previous study, we identified the third intracellular loop of the M3R as the region responsible for the interaction with the Gβ_5−RGS7 complex (*30*). We found that deletion of this loop rendered the M3R insensitive to the Gβ_5−RGS7 complex, while recombinant M3Ri3 could directly bind to the isolated DEP domain or the RGS7 monomer. Interestingly, the full-length Gβ_5−RGS7 dimer could not bind to M3Ri3 in vitro, which made it difficult to explain how the dimer could inhibit M3R signaling. We hypothesized that the Gβ_5−RGS7 can bind to the M3R after assuming the open conformation, the notion supported in this paper (Figures 3 and 6A). We also reasoned that mutations that facilitate binding of the Gβ_5−RGS7 complex to M3Ri3 should improve the apparent effectiveness of the Gβ_5−RGS7 complex as an inhibitor of M3R signaling. However, our assays did not detect such an enhanced activity (Figure 4).

To explain the similarity between the wild-type and mutant Gβ_5−RGS7 complexes in their ability to inhibit M3R signaling, we extended our model. We postulated that the receptor has an intrinsic capacity to induce the open conformation in the Gβ_5−RGS7 complex and that this capability is associated with an M3R region that is distinct from the third loop. This prediction proved to be correct: we found that the C-tail of the receptor can interact with the Gβ_5−RGS7 complex (Figures 5 and 6). Truncation of the C-terminus rendered the M3R insensitive to the inhibition by the wild-type Gβ_5−RGS7 complex, but interestingly, the open Gβ_5−RGS7 mutant could inhibit the truncated receptor (Figure 5). In other words, the Gβ_5−RGS7 molecule that has already been opened by a mutation does not require the M3R C-tail to do so.

Our data show that the isolated C-tail cannot bind to the wild-type Gβ_5−RGS7 complex but does bind the open mutant, which implies synergy between the C-tail and the third intracellular loop in the process of Gβ_5−RGS7 complex recruitment. Gβ_5 binds to the C-tail of the M3R in a selective manner, indicating that it associates with the sequence unique for the M3 subtype. The C-tail of the M3R can now be added to the list of putative binding partners of Gβ_5, in addition to Gαi and PLC, which in early studies were shown to interact with G$\beta_5\gamma_2$ (*47*−*50*). On the other hand, the DEP domain of RGS7 appears to bind to both the C-tail and M3Ri3. A more detailed structure−function analysis will be needed to further dissect molecular events involved in the interaction of the M3R with the Gβ_5−RGS7 complex. Since M3R can oligomerize (*51*), it is possible that the Gβ_5−RGS7 complex, being a rather large molecule, can simultaneously bind to the C-tail of one M3R molecule and the third loop of another.

Interaction of the M3R with the Gβ_5−RGS7 complex supports the emerging concept that GPCRs can form complexes with RGS proteins (*52*−*56*). For example, yeast RGS protein Sst2 that is unrelated to the R7 family can directly bind to GPCR Ste2 (*57*). That study is particularly interesting in relation to this work because the Ste2−Sst2 interaction requires the C-tail of the Ste2 receptor and the DEP domain present in Sst2. The results of another group indicated that RGS9 also associated via its DEP domain with the dopamine D2 receptor (*58*). Our current paper extends our understanding of the role of the DEP and Gβ_5/GGL entities in the R7 family by showing that their dissociation in the Gβ_5−RGS7 complex can facilitate its interaction with the M3R. The identification of the M3R C-terminus as the site essential for the interaction with the Gβ_5−RGS7 complex provides additional mechanistic insight into the interaction between this receptor and the Gβ_5−RGS7 complex.

ACKNOWLEDGMENT

We thank Dr. Andrew Tobin (University of Leicester) for DNA constructs.

REFERENCES

1. Limbird, L. E., Gill, D. M., and Lefkowitz, R. J. (1980) Agonist-promoted coupling of the β-adrenergic receptor with the guanine nucleotide regulatory protein of the adenylate cyclase system. *Proc. Natl. Acad. Sci. U.S.A. 77*, 775–779.
2. Fung, B. K., Hurley, J. B., and Stryer, L. (1981) Flow of information in the light-triggered cyclic nucleotide cascade of vision. *Proc. Natl. Acad. Sci. U.S.A. 78*, 152–156.
3. Northup, J. K., Smigel, M. D., Sternweis, P. C., and Gilman, A. G. (1983) The subunits of the stimulatory regulatory component of adenylate cyclase. Resolution of the activated 45,000-dalton (α) subunit. *J. Biol. Chem. 258*, 11369–11376.
4. Clapham, D. E., and Neer, E. J. (1993) New roles for G-protein $\beta\gamma$-dimers in transmembrane signalling. *Nature 365*, 403–406.
5. Neer, E. J., and Clapham, D. E. (1988) Roles of G protein subunits in transmembrane signalling. *Nature 333*, 129–134.
6. Smrcka, A. V. (2008) G protein $\beta\gamma$ subunits: Central mediators of G protein-coupled receptor signaling. *Cell. Mol. Life Sci. 65*, 2191–2214.
7. Dohlman, H. G., and Thorner, J. (1997) RGS proteins and signaling by heterotrimeric G proteins. *J. Biol. Chem. 272*, 3871–3874.
8. Berman, D. M., and Gilman, A. G. (1998) Mammalian RGS proteins: Barbarians at the gate. *J. Biol. Chem. 273*, 1269–1272.
9. Hepler, J. R. (1999) Emerging roles for RGS proteins in cell signalling. *Trends Pharmacol. Sci. 20*, 376–382.
10. Chidiac, P., and Roy, A. A. (2003) Activity, regulation, and intracellular localization of RGS proteins. *Recept. Channels 9*, 135–147.
11. Willars, G. B. (2006) Mammalian RGS proteins: Multifunctional regulators of cellular signalling. *Semin. Cell Dev. Biol. 17*, 363–376.
12. Witherow, D. S., and Slepak, V. Z. (2003) A Novel Kind of G Protein Heterodimer: The Gβ5-RGS Complex. *Recept. Channels 9*, 205–212.
13. Anderson, G. R., Posokhova, E., and Martemyanov, K. A. (2009) The R7 RGS protein family: Multi-subunit regulators of neuronal G protein signaling. *Cell Biochem. Biophys. 54*, 33–46.
14. Slepak, V. Z. (2009) Structure, Function, and Localization of Gβ5-RGS Complexes. In Progress in Molecular Biology and Translational Science (Fisher, R. A., Ed.) Vol. *86*, pp 157−203, Academic Press, New York.
15. Cabrera, J. L., de Freitas, F., Satpaev, D. K., and Slepak, V. Z. (1998) Identification of the Gβ5-RGS7 protein complex in the retina. *Biochem. Biophys. Res. Commun. 249*, 898–902.
16. Levay, K., Cabrera, J. L., Satpaev, D. K., and Slepak, V. Z. (1999) Gβ5 prevents the RGS7-Gαo interaction through binding to a distinct Gγ-like domain found in RGS7 and other RGS proteins. *Proc. Natl. Acad. Sci. U.S.A. 96*, 2503–2507.
17. Snow, B. E., Krumins, A. M., Brothers, G. M., Lee, S. F., Wall, M. A., Chung, S., Mangion, J., Arya, S., Gilman, A. G., and Siderovski, D. P. (1998) A G protein γ subunit-like domain shared between RGS11 and other RGS proteins specifies binding to Gβ5 subunits. *Proc. Natl. Acad. Sci. U.S.A. 95*, 13307–13312.
18. Drenan, R. M., Doupnik, C. A., Boyle, M. P., Muglia, L. J., Huettner, J. E., Linder, M. E., and Blumer, K. J. (2005) Palmitoylation regulates plasma membrane-nuclear shuttling of R7BP, a novel membrane anchor for the RGS7 family. *J. Cell Biol. 169*, 623–633.
19. Martemyanov, K. A., Yoo, P. J., Skiba, N. P., and Arshavsky, V. Y. (2005) R7BP, a novel neuronal protein interacting with RGS proteins of the R7 family. *J. Biol. Chem. 280*, 5133–5136.
20. Jayaraman, M., Zhou, H., Jia, L., Cain, M. D., and Blumer, K. J. (2008) R9AP and R7BP: traffic cops for the RGS7 family in phototransduction and neuronal GPCR signaling. *Trends Pharmacol. Sci. 30*, 17–24.

21. Narayanan, V., Sandiford, S. L., Wang, Q., Keren-Raifman, T., Levay, K., and Slepak, V. Z. (2007) Intramolecular Interaction between the DEP Domain of RGS7 and the Gβ_5 Subunit. *Biochemistry 46*, 6859–6870.
22. Cheever, M. L., Snyder, J. T., Gershburg, S., Siderovski, D. P., Harden, T. K., and Sondek, J. (2008) Crystal structure of the multifunctional Gβ5-RGS9 complex. *Nat. Struct. Mol. Biol. 15*, 155–162.
23. Hooks, S. B., Martemyanov, K., and Zachariou, V. (2008) A role of RGS proteins in drug addiction. *Biochem. Pharmacol. 75*, 76–84.
24. Hooks, S. B., Waldo, G. L., Corbitt, J., Bodor, E. T., Krumins, A. M., and Harden, T. K. (2003) RGS6, RGS7, RGS9, and RGS11 stimulate GTPase activity of Gi family G-proteins with differential selectivity and maximal activity. *J. Biol. Chem. 278*, 10087–10093.
25. Hajdu-Cronin, Y. M., Chen, W. J., Patikoglou, G., Koelle, M. R., and Sternberg, P. W. (1999) Antagonism between $G_o\alpha$ and $G_q\alpha$ in *Caenorhabditis elegans*: The RGS protein EAT-16 is necessary for $G_o\alpha$ signaling and regulates $G_q\alpha$ activity. *Genes Dev. 13*, 1780–1793.
26. Chase, D. L., Patikoglou, G. A., and Koelle, M. R. (2001) Two RGS proteins that inhibit $G\alpha_o$ and $G\alpha_q$ signaling in *C. elegans* neurons require a Gβ_5-like subunit for function. *Curr. Biol. 11*, 222–231.
27. Patikoglou, G. A., and Koelle, M. R. (2002) An N-terminal region of *Caenorhabditis elegans* RGS proteins EGL-10 and EAT-16 directs inhibition of Gαo versus Gαq signaling. *J. Biol. Chem. 277*, 47004–47013.
28. Witherow, D. S., Wang, Q., Levay, K., Cabrera, J. L., Chen, J., Willars, G. B., and Slepak, V. Z. (2000) Complexes of the G protein subunit gβ5 with the regulators of G protein signaling RGS7 and RGS9. Characterization in native tissues and in transfected cells. *J. Biol. Chem. 275*, 24872–24880.
29. Witherow, D. S., Tovey, S. C., Wang, Q., Willars, G. B., and Slepak, V. Z. (2003) Gβ5·RGS7 inhibits Gαq-mediated signaling via a direct protein-protein interaction. *J. Biol. Chem. 278*, 21307–21313.
30. Sandiford, S., and Slepak, V. (2009) Gβ5-RGS7 selectively inhibits muscarinic M3 receptor signaling via the interaction between the third intracellular loop of the receptor and the DEP domain of RGS7. *Biochemistry 48*, 2282–2289.
31. Wess, J., Brann, M. R., and Bonner, T. I. (1989) Identification of a small intracellular region of the muscarinic m3 receptor as a determinant of selective coupling to PI turnover. *FEBS Lett. 258*, 133–136.
32. Wu, G., Krupnick, J. G., Benovic, J. L., and Lanier, S. M. (1997) Interaction of arrestins with intracellular domains of muscarinic and α2-adrenergic receptors. *J. Biol. Chem. 272*, 17836–17842.
33. Wu, G., Benovic, J. L., Hildebrandt, J. D., and Lanier, S. M. (1998) Receptor docking sites for G-protein $\beta\gamma$ subunits. Implications for signal regulation. *J. Biol. Chem. 273*, 7197–7200.
34. Wu, G., Bogatkevich, G. S., Mukhin, Y. V., Benovic, J. L., Hildebrandt, J. D., and Lanier, S. M. (2000) Identification of G$\beta\gamma$ binding sites in the third intracellular loop of the M(3)-muscarinic receptor and their role in receptor regulation. *J. Biol. Chem. 275*, 9026–9034.
35. Lucas, J. L., Wang, D., and Sadee, W. (2006) Calmodulin binding to peptides derived from the i3 loop of muscarinic receptors. *Pharm. Res. 23*, 647–653.
36. Simon, V., Guidry, J., Gettys, T. W., Tobin, A. B., and Lanier, S. M. (2006) The proto-oncogene SET interacts with muscarinic receptors and attenuates receptor signaling. *J. Biol. Chem. 281*, 40310–40320.
37. Budd, D. C., McDonald, J. E., and Tobin, A. B. (2000) Phosphorylation and regulation of a Gq/11-coupled receptor by casein kinase 1α. *J. Biol. Chem. 275*, 19667–19675.
38. Luo, J., Busillo, J. M., and Benovic, J. L. (2008) M3 muscarinic acetylcholine receptor-mediated signaling is regulated by distinct mechanisms. *Mol. Pharmacol. 74*, 338–347.
39. Witherow, D. S., and Slepak, V. Z. (2004) Biochemical purification and functional analysis of complexes between the G-protein subunit Gβ5 and RGS proteins. *Methods Enzymol. 390*, 149–162.
40. Budd, D. C., McDonald, J., Emsley, N., Cain, K., and Tobin, A. B. (2003) The C-terminal tail of the M3-muscarinic receptor possesses anti-apoptotic properties. *J. Biol. Chem. 278*, 19565–19573.
41. Guex, N., and Peitsch, M. C. (1997) SWISS-MODEL and the Swiss-PdbViewer: An environment for comparative protein modeling. *Electrophoresis 18*, 2714–2723.
42. Guex, N., Peitsch, M. C., and Schwede, T. (2009) Automated comparative protein structure modeling with SWISS-MODEL and Swiss-PdbViewer: A historical perspective. *Electrophoresis 30* (Suppl. 1), S162–S173.
43. Civera, C., Simon, B., Stier, G., Sattler, M., and Macias, M. J. (2005) Structure and dynamics of the human pleckstrin DEP domain: Distinct molecular features of a novel DEP domain subfamily. *Proteins 58*, 354–366.
44. Brady, A. E., and Limbird, L. E. (2002) G protein-coupled receptor interacting proteins: Emerging roles in localization and signal transduction. *Cell. Signalling 14*, 297–309.
45. Bockaert, J., Fagni, L., Dumuis, A., and Marin, P. (2004) GPCR interacting proteins (GIP). *Pharmacol. Ther. 103*, 203–221.
46. Chen, C. K., Eversole-Cire, P., Zhang, H., Mancino, V., Chen, Y. J., He, W., Wensel, T. G., and Simon, M. I. (2003) Instability of GGL domain-containing RGS proteins in mice lacking the G protein β-subunit Gβ5. *Proc. Natl. Acad. Sci. U.S.A. 100*, 6604–6609.
47. Watson, A. J., Katz, A., and Simon, M. I. (1994) A fifth member of the mammalian G-protein β-subunit family. Expression in brain and activation of the β2 isotype of phospholipase C. *J. Biol. Chem. 269*, 22150–22156.
48. Watson, A. J., Aragay, A. M., Slepak, V. Z., and Simon, M. I. (1996) A novel form of the G protein β subunit Gβ5 is specifically expressed in the vertebrate retina. *J. Biol. Chem. 271*, 28154–28160.
49. Zhang, S., Coso, O. A., Lee, C., Gutkind, J. S., and Simonds, W. F. (1996) Selective activation of effector pathways by brain-specific G protein β5. *J. Biol. Chem. 271*, 33575–33579.
50. Yoshikawa, D. M., Hatwar, M., and Smrcka, A. V. (2000) G protein β5 subunit interactions with α subunits and effectors. *Biochemistry 39*, 11340–11347.
51. Zeng, F., and Wess, J. (2000) Molecular aspects of muscarinic receptor dimerization. *Neuropsychopharmacology 23*, S19–S31.
52. Bernstein, L. S., Ramineni, S., Hague, C., Cladman, W., Chidiac, P., Levey, A. I., and Hepler, J. R. (2004) RGS2 binds directly and selectively to the M1 muscarinic acetylcholine receptor third intracellular loop to modulate Gq/11α signaling. *J. Biol. Chem. 279*, 21248–21256.
53. Georgoussi, Z., Leontiadis, L., Mazarakou, G., Merkouris, M., Hyde, K., and Hamm, H. (2006) Selective interactions between G protein subunits and RGS4 with the C-terminal domains of the μ- and δ-opioid receptors regulate opioid receptor signaling. *Cell. Signalling 18*, 771–782.
54. Schwendt, M., and McGinty, J. F. (2007) Regulator of G-protein signaling 4 interacts with metabotropic glutamate receptor subtype 5 in rat striatum: Relevance to amphetamine behavioral sensitization. *J. Pharmacol. Exp. Ther. 323*, 650–657.
55. Langer, I., Tikhonova, I. G., Boulegue, C., Esteve, J. P., Vatinel, S., Ferrand, A., Moroder, L., Robberecht, P., and Fourmy, D. (2009) Evidence for a direct and functional interaction between the regulators of G protein signaling-2 and phosphorylated C terminus of cholecystokinin-2 receptor. *Mol. Pharmacol. 75*, 502–513.
56. Abramow-Newerly, M., Roy, A. A., Nunn, C., and Chidiac, P. (2006) RGS proteins have a signalling complex: Interactions between RGS proteins and GPCRs, effectors, and auxiliary proteins. *Cell. Signalling 18*, 579–591.
57. Ballon, D. R., Flanary, P. L., Gladue, D. P., Konopka, J. B., Dohlman, H. G., and Thorner, J. (2006) DEP-domain-mediated regulation of GPCR signaling responses. *Cell 126*, 1079–1093.
58. Kovoor, A., Seyffarth, P., Ebert, J., Barghshoon, S., Chen, C. K., Schwarz, S., Axelrod, J. D., Cheyette, B. N., Simon, M. I., Lester, H. A., and Schwarz, J. (2005) D2 dopamine receptors colocalize regulator of G-protein signaling 9-2 (RGS9-2) via the RGS9 DEP domain, and RGS9 knock-out mice develop dyskinesias associated with dopamine pathways. *J. Neurosci. 25*, 2157–2165.